AIAA JOURNAL
Vol. 44, No. 7, July 2006

Three-Dimensional Analysis of Wrinkled Membranes Using Modification Scheme of Stress-Strain Tensor

Kyoichi Nakashino*
Tokai University, Kanagawa 259-1292, Japan
and
M. C. Natori†
Institute of Space and Astronautical Science, Japan Aerospace Exploration Agency, Kanagawa 229-8510, Japan

DOI: 10.2514/1.12052

Three-dimensional finite element analysis using conventional membrane elements tends to be numerically unstable because of their lack of bending stiffness. Additionally, membrane structures are highly susceptible to localized buckling, posing further numerical difficulties. In this paper, a modified stress-strain tensor, recently proposed by the authors to account for membrane wrinkling, is applied to three-dimensional finite element analysis of membrane structures with the aim to overcome the preceding numerical difficulties. It is found through numerical investigations that the use of the modified stress-strain tensor renders the iterative solution process remarkably stable, and enables one to obtain the converged solution for those problems that are difficult to solve using conventional membrane elements.

Nomenclature

$\boldsymbol{C}$ = stress-strain tensor assumed between $\boldsymbol{S}$ and $\boldsymbol{E}$
$\boldsymbol{C}'$ = modified stress-strain tensor
$\boldsymbol{E}$ = Green–Lagrange strain tensor
E = Young's modulus
$\boldsymbol{F}$ = deformation gradient tensor
$\boldsymbol{f}$ = external force vector
$\boldsymbol{K}$ = tangent stiffness matrix
$\boldsymbol{Q}$ = internal force vector
$\boldsymbol{S}$ = second Piola–Kirchhoff stress tensor
$\boldsymbol{u}^n$ = nodal displacements at nth iteration
t = thickness of membrane
$\boldsymbol{w}$ = unit vector transverse to wrinkling direction
β = physical amount of wrinkliness
μ = stabilization factor
ν = Poisson's ratio
$\boldsymbol{\sigma}$ = Cauchy stress tensor
$\dot{}$ = material time derivative
$'$ = variables modified to account for wrinkling
$\{\cdot\}$ = second-order tensor expressed in column vector form
$[\cdot]$ = fourth-order tensor expressed in matrix form

I. Introduction

CURRENTLY, thin membranes are attracting increasing interest as structural components of large lightweight space structures. Examples include solar sails, sunshields, and inflatable parabolic reflectors. Unlike other semirigid structural components, such as plates or shells, membranes have little resistance against compression. As a result, membrane structures are highly susceptible to localized buckling, or wrinkling. Because wrinkling of thin membranes causes strong nonlinearities in their structural responses, the phenomenon should be modeled in a proper manner.

A suitable way to treat wrinkled membranes is provided by the tension field (TF) theory [1]. In the TF theory, a thin membrane is idealized as a membrane with zero bending stiffness. Theoretically, such an idealized membrane cannot sustain any compressive stresses, and therefore when compressive stresses are about to appear in the membrane, they are immediately released by out-of-plane deformations, resulting in fine wrinkling of the membrane. Accordingly, wrinkled regions of the membrane are supposed to be in uniaxial tension state, where stresses perpendicular to wrinkle lines equal zero.

Since the early 1970s, many studies have been conducted on the finite element analysis of partly wrinkled membranes in the light of the TF theory [2–6]. In these studies, wrinkling is usually accounted for by modifying the stress-strain relation of membranes. Most notable is the modification of the elasticity matrix proposed by Miller et al. [2]. In their approach, the elasticity matrix of each membrane element is iteratively modified according to current estimates of the stress state; the process is continued until desired convergence is achieved. The approach was validated through analytical solutions, and has been successfully used for analysis of partly wrinkled membrane structures [7–9]. However, convergence problems may exist with this approach, because nonlinearities originated from wrinkling are not taken into account in a fully consistent manner.

Roddeman et al. [10] developed an alternative model of wrinkled membranes, where wrinkling is accounted for by modifying the deformation gradient tensor of membranes. Since then, several researchers applied the Roddeman model to finite element analysis of partly wrinkled membrane structures, using various techniques [11–14]. Finite element implementation of the Roddeman model has been further developed by Lu et al. [15], who, for the first time, derived explicit formulas for the tangent stiffness matrix that is fully consistent with the Roddeman model. A similar study has been made by Schoop et al. [16], where the consistent tangent stiffness matrix was derived in a different fashion. Recently, the authors have shown that the modification of the deformation gradient tensor in the Roddeman model can be replaced by a formal modification of the stress-strain tensor [17]. The modified stress-strain tensor automatically leads to the consistent tangent stiffness matrix, saving complicated calculation procedures. They have also shown that the use of the modified stress-strain tensor provides good convergence

Received 7 July 2004; revision received 30 December 2005; accepted for publication 12 January 2006.

*Assistant Professor, Department of Aeronautics and Astronautics, 1117 Kitakaname, Hiratsuka; nakasino@keyaki.cc.u-tokai.ac.jp. Member AIAA.
†Professor, Space Structures and Materials, 3-1-1 Yoshinodai, Sagamihara, Associate Fellow AIAA.

properties to the iterative solution process of two-dimensional wrinkling analysis.

In the preceding studies, the TF theory was used for the purpose of accounting for the wrinkling response of membranes, and naturally, the interest of researchers was focused on a reasonable evaluation of the stress field of wrinkled membranes. In the present paper, however, the TF theory is used for a rather different purpose. More specifically, we use the theory as a means to circumvent instabilities encountered in three-dimensional finite element analysis of membrane structures.

Finite element analysis using conventional membrane elements is inherently unstable because of the following two reasons:

1) Membrane elements have no bending rigidity. As a result, membrane elements, when not tensioned, do not posses any out-of-plane stiffness, leading to instability of underconstrained conditions [18]. In the finite element context, this instability is observed as zero eigenvalues of the tangent stiffness matrix.

2) The presence of compressive stresses renders the potential energy of membranes nonconvex [19]. Consequently, convergence of the nonlinear solution is not guaranteed when conventional Newton–Raphson scheme is employed, as a result of which instability problems are likely to occur during the iterative solution process. In the finite element context, this instability is observed as nonpositive definiteness of the tangent stiffness matrix.

The former instability can be averted with relative ease, for example, by quasistatic analysis, where artificial damping is introduced for the stabilization. For this purpose, even more sophisticated techniques are available, such as the dynamic relaxation method [20,21]. In the present study, this type of instability is treated by a relatively simple technique, which will be discussed in Sec. III. In contrast, the latter instability is much more difficult to deal with. One possibility to overcome this instability is to preserve the positive definiteness of the tangent stiffness matrix by eliminating compressive stresses of membranes. However, such elimination is difficult to perform in a mechanically consistent manner. It is at this point that the TF theory is expected to provide the solution. In the TF theory, compressive stresses are eliminated through modifications of either the stress-strain relation or the kinematic description of membranes. It is thus expected that the tangent stiffness matrix evaluated based on the TF theory will preserve the positive definiteness, leading to stable solution process.

In the present paper, the preceding expectation is examined through three-dimensional finite element analysis of membrane structures, where the TF theory is incorporated by using the modified stress-strain tensor recently proposed by the authors. The results are then compared with those obtained using conventional membrane elements that allow compressive stresses. The comparative study reveals that the use of the modified stress-strain tensor stabilizes and improves the iterative process remarkably.

The remainder of the paper is organized as follows: In Sec. II, Roddeman's wrinkling model is briefly reviewed, followed by the description of the modification scheme of the stress-strain tensor proposed by the authors. Section III deals with finite element implementation issues, including the treatment of wrinkling and the stabilization technique for the instability resulting from underconstrained conditions. In Sec. IV, two numerical examples are treated to investigate the stabilizing effect of the modified stress-strain tensor.

II. Wrinkling Model Based on the TF Theory

A. Roddeman Model

Roddeman et al. [10] have proposed a wrinkling model in which the deformation gradient tensor in wrinkled regions of membranes is modified so that the stress field in these regions becomes consistent with the TF theory. Formulations of Roddeman's wrinkling model are briefly reviewed next.

Consider a small part of wrinkled membrane shown in Fig. 1. The wrinkling direction is dictated by a unit vector, of which direction is perpendicular to the wrinkle lines. The fine shape of the wrinkled membrane, formally drawn in the figure, cannot be uniquely determined because of the "no bending stiffness" assumption in the TF theory. Alternatively, we attempt to approximate the deformation of the wrinkled membrane by a pseudomean surface (a dotted rectangle in Fig. 1), and denote the corresponding deformation gradient tensor by $\boldsymbol{F}$. Because the deformation gradient ignores the out-of-plane deformation of the wrinkled membrane, it should be modified as

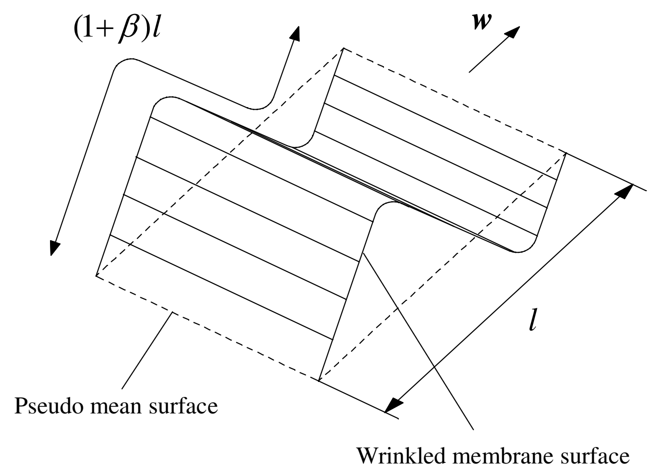

Fig. 1 Wrinkled membrane.

$$\boldsymbol{F}' = (\boldsymbol{I} + \beta \boldsymbol{w} \otimes \boldsymbol{w}) \cdot \boldsymbol{F} \tag{1}$$

where $\boldsymbol{I}$ denotes the identity tensor (see Fig. 1). Using the modified deformation gradient, the Green–Lagrange strain of the wrinkled membrane is obtained as

$$\boldsymbol{E}' = \frac{1}{2}(\boldsymbol{F}'^T \cdot \boldsymbol{F}' - \boldsymbol{I}) \tag{2}$$

The second Piola–Kirchhoff stress of the wrinkled membrane may be obtained by the following constitutive equation:

$$\boldsymbol{S}' = \boldsymbol{C}{:}\boldsymbol{E}' \tag{3}$$

The Cauchy stress of the wrinkled membrane is given as

$$\boldsymbol{\sigma}' = \frac{1}{\det \boldsymbol{F}'} \boldsymbol{F}' \cdot \boldsymbol{S}' \cdot \boldsymbol{F}'^T \tag{4}$$

In the TF theory, wrinkled membranes are supposed to be in uniaxial tension state. As a result, the Cauchy stress in the $\boldsymbol{w}$ direction should vanish, and the following condition must hold:

$$\boldsymbol{\sigma}' \cdot \boldsymbol{w} = \boldsymbol{0} \tag{5}$$

The variables β and $\boldsymbol{w}$, introduced in Eq. (1), are determined so that the preceding condition is satisfied. Having obtained β and $\boldsymbol{w}$, we can evaluate the strains and stresses in the wrinkled membrane by Eqs. (2) and (3).

B. Modification Scheme of Stress-Strain Tensor for Wrinkled Membranes

In its original form, the Roddeman model modifies the deformation gradient tensor of the wrinkled membrane. The local strains and stresses of the membrane are evaluated through the modified deformation gradient tensor. To apply the Roddeman model to nonlinear finite element analysis, we must calculate the Green–Lagrange strain, as well as its rate counterparts, such as $\dot{\boldsymbol{E}}'$ and $(\delta \boldsymbol{E}')^{\cdot}$, where δ signifies the variation due to the virtual displacements. The calculation of the preceding quantities, however, requires rather complicated procedures.

In [17], the authors have shown that the modification of the deformation gradient tensor in the Roddeman model can be replaced by a formal modification of the stress-strain tensor, and presented explicit formulas for the modified stress-strain tensor. An advantage of this modified stress-strain tensor is that it automatically leads to the consistent tangent stiffness matrix, where nonlinearities originated from wrinkling are taken into account. In the literature, there are two other approaches proposed for the calculation of the consistent tangent stiffness matrix [15,16]. However, modifying the stress-strain tensor provides a much simpler calculation. Next, we summarize the modification scheme of the stress-strain tensor for wrinkled membranes.

For the equations to be presented in a concise manner, we define the following vectors and matrices.

$$\{\boldsymbol{E}\} = [E_{11} \quad E_{22} \quad 2E_{12}]^T \tag{6a}$$

$$\boldsymbol{n}_1 = [n_1 n_1 \quad n_2 n_2 \quad 2n_1 n_2]^T \tag{6b}$$

$$\boldsymbol{n}_2 = [m_1 n_1 \quad m_2 n_2 \quad m_1 n_2 + m_2 n_1]^T \tag{6c}$$

$$\boldsymbol{n}_3 = [m_1 m_1 \quad m_2 m_2 \quad 2m_1 m_2]^T \tag{6d}$$

$$[\boldsymbol{C}] = \begin{bmatrix} C^{1111} & C^{1122} & C^{1112} \\ C^{2211} & C^{2222} & C^{2212} \\ C^{1211} & C^{1222} & C^{1212} \end{bmatrix} \tag{6e}$$

where the $E_{\alpha\beta}$ represent the covariant components of the usual Green–Lagrange strain and $C^{\alpha\beta\xi\eta}$ the contravariant components of the usual stress-strain tensor. The m_α and n_α are functions of an unknown parameter θ, defined as

$$m_1 = -\sin\theta, \qquad m_2 = \cos\theta \tag{7}$$

$$n_1 = \cos\theta, \qquad n_2 = \sin\theta \tag{8}$$

The parameter θ is determined by solving the following nonlinear equation, which corresponds to Eq. (5) in the Roddeman model [15].

$$f(\theta) = \boldsymbol{n}_2^T \cdot [\boldsymbol{C}] \cdot \{\boldsymbol{E}\} + \gamma \boldsymbol{n}_2^T \cdot [\boldsymbol{C}] \cdot \boldsymbol{n}_1 = 0 \tag{9}$$

where

$$\gamma = -\frac{\boldsymbol{n}_1^T \cdot [\boldsymbol{C}] \cdot \{\boldsymbol{E}\}}{\boldsymbol{n}_1^T \cdot [\boldsymbol{C}] \cdot \boldsymbol{n}_1} \tag{10}$$

Equation (9) contains only one unknown variable θ, and is easily solved by an appropriate numerical method. Once the parameter θ is obtained, the modified stress-strain tensor can be calculated by the following formula:

$$[\boldsymbol{C}'] = [\boldsymbol{C}] - \frac{1}{\boldsymbol{n}_1^T \cdot [\boldsymbol{C}] \cdot \boldsymbol{n}_1} [\boldsymbol{C}] \cdot \boldsymbol{n}_1 \cdot \boldsymbol{n}_1^T \cdot [\boldsymbol{C}] + \frac{2\gamma}{\partial f / \partial \theta} [\boldsymbol{C}] \cdot \boldsymbol{b} \cdot \boldsymbol{b}^T \cdot [\boldsymbol{C}] \tag{11}$$

where

$$\boldsymbol{b} = \boldsymbol{n}_2 - \frac{\boldsymbol{n}_1^T \cdot [\boldsymbol{C}] \cdot \boldsymbol{n}_2}{\boldsymbol{n}_1^T \cdot [\boldsymbol{C}] \cdot \boldsymbol{n}_1} \boldsymbol{n}_1 \tag{12}$$

The derivative $\partial f / \partial \theta$ appearing in Eq. (11) may be obtained by

$$\frac{\partial f}{\partial \theta} = \boldsymbol{n}_3^T \cdot [\boldsymbol{C}] \cdot (\{\boldsymbol{E}\} + \gamma \boldsymbol{n}_1) + 2\gamma \left[\boldsymbol{n}_2^T \cdot [\boldsymbol{C}] \cdot \boldsymbol{n}_2 - \frac{(\boldsymbol{n}_1^T \cdot [\boldsymbol{C}] \cdot \boldsymbol{n}_2)^2}{\boldsymbol{n}_1^T \cdot [\boldsymbol{C}] \cdot \boldsymbol{n}_2} \right] \tag{13}$$

III. Finite Element Implementation

A. Treatment of Wrinkling

In the finite element calculations, the tangent stiffness matrix and the internal force vector for each element are usually obtained by Gauss numerical integration, where stresses, strains and other related quantities are evaluated at each integration point. In case the membranes are partly wrinkled or slackened, we must properly evaluate the preceding quantities, at each integration point, in accordance with the state of the membrane (i.e., taut, wrinkled, or slackened). This can be accomplished by modifying the usual stress-strain tensor according to

$$\text{taut}: [\boldsymbol{C}] \Rightarrow [\boldsymbol{C}] \tag{14a}$$

$$\text{wrinkled}: [\boldsymbol{C}] \Rightarrow [\boldsymbol{C}'] \tag{14b}$$

$$\text{slackened}: [\boldsymbol{C}] \Rightarrow [\boldsymbol{O}] \tag{14c}$$

where $[\boldsymbol{O}]$ denotes a 3×3 zero matrix. The state of the membrane can be determined by the mixed stress-strain criterion, which has been adopted in many studies. Detailed explanation of the mixed stress-strain criterion is found in [3,22]. Equations (14) establish the treatment of wrinkling used in the present study.

B. Instability Problem of Underconstrained Conditions

Generally, membrane elements have no bending rigidity. As a result, membrane elements without tensile stresses do not posses any out-of-plane stiffness [18]. This lack of stiffness leads to the singularity of the tangent stiffness matrix, in particular when an initial estimated configuration of the membrane is in tension free state. To overcome this singularity problem, we adopt the following simple approach.

In nonlinear finite element calculations, the equilibrium equation to be solved is expressed as

$$\boldsymbol{Q}(\boldsymbol{u}) = \boldsymbol{f} \tag{15}$$

Here we write the internal force vector as $Q(u)$, because Q is a nonlinear function of the nodal displacements u. For simplicity, we assume here that $\boldsymbol{f}$ is independent of $\boldsymbol{u}$. The solution $\boldsymbol{u}$ to Eq. (15) can be obtained by the Newton–Raphson iteration scheme, the nth step of which is described as

$$\boldsymbol{K} \cdot (\boldsymbol{u}^{n+1} - \boldsymbol{u}^n) = \boldsymbol{f} - \boldsymbol{Q}(\boldsymbol{u}^n) \tag{16}$$

where

$$\boldsymbol{K} \equiv \left. \frac{\partial \boldsymbol{Q}(\boldsymbol{u})}{\partial \boldsymbol{u}} \right|_{\boldsymbol{u}=\boldsymbol{u}^n} \tag{17}$$

represents the tangent stiffness matrix, and $\boldsymbol{u}^n$ an approximated value of the solution at the nth iteration. In case that the matrix $\boldsymbol{K}$ is singular and not invertible, Eq. (16) cannot be solved for $\boldsymbol{u}^{n+1}$, and thus the iteration process fails. To circumvent this problem, we introduce a stabilization factor (>0), and replace Eq. (16) by

$$(\boldsymbol{K} + \mu \boldsymbol{I}) \cdot (\boldsymbol{u}^{n+1} - \boldsymbol{u}^n) = \boldsymbol{f} - \boldsymbol{Q}(\boldsymbol{u}^n) \tag{18}$$

where $\boldsymbol{I}$ represents the unit matrix. The value of μ is specified by the analyst so that the matrix $(\boldsymbol{K} + \mu \boldsymbol{I})$ becomes numerically invertible.

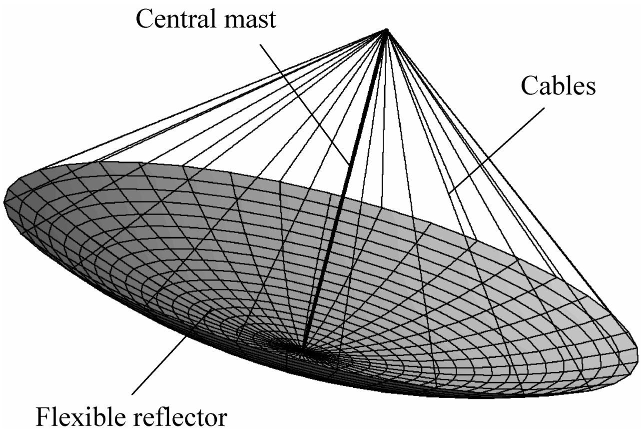

Fig. 2 Conceptual sketch of the spin-stabilized antenna system.

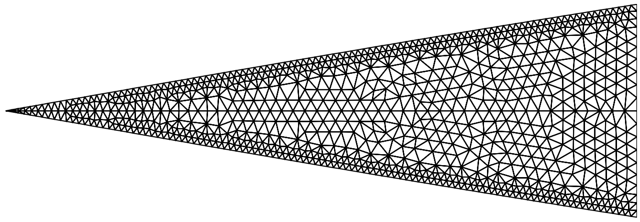

Fig. 3 Finite element model of a single gore.

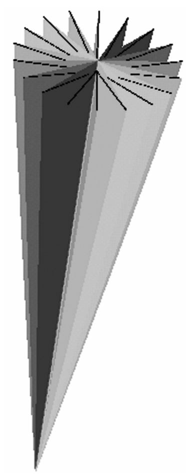

Fig. 4 Initial configuration of the spin-stabilized antenna system.

The solution $\boldsymbol{u}$ of the original Eq. (15) is obtained when the iterative scheme (18) converges (i.e., $\boldsymbol{u}^{n+1} - \boldsymbol{u}^{n} \rightarrow \mathbf{0}$). In our numerical calculations, the stabilization factor is gradually decreased to accelerate the solution process, and eventually is set to zero, when μ falls below a certain threshold value.

IV. Numerical Examples

A. Example 1: Spin-Stabilized Antenna System

An idea has been proposed to construct a large space antenna system, of which a reflector, composed of very flexible members, is stabilized by centrifugal forces [23,24]. A conceptual sketch of this antenna system, which we call here the spin-stabilized antenna system, is shown in Fig. 2. The antenna structure maintains its rotational motion around a central mast, generating centrifugal forces by which a flexible membrane reflector is stabilized. The outer rim of the reflector is connected to the mast with several cables. A static analysis of this antenna system is considered here.

A numerical model of the reflector is composed of 18 identical gores, each forming a developable surface. The gore shape is determined so that the paraboloidal surface, 400 m aperture with a focal length to diameter ratio $(f/d) = 0.5$, is approximated when all the gores are seamed together in the unstrained condition. A finite element model of a single gore is shown in Fig. 3. The model is composed of 1648 linear triangular membrane elements. Finer meshes are adapted along the radial boundaries to reduce the spatial discretization error of the profile. The cables attached to the antenna system are modeled as constraint conditions with the endpoints of each cable maintained at a prescribed distance (i.e., a natural length of the cable). These constraints are activated only when the distance between the two endpoints exceeds the prescribed value, or

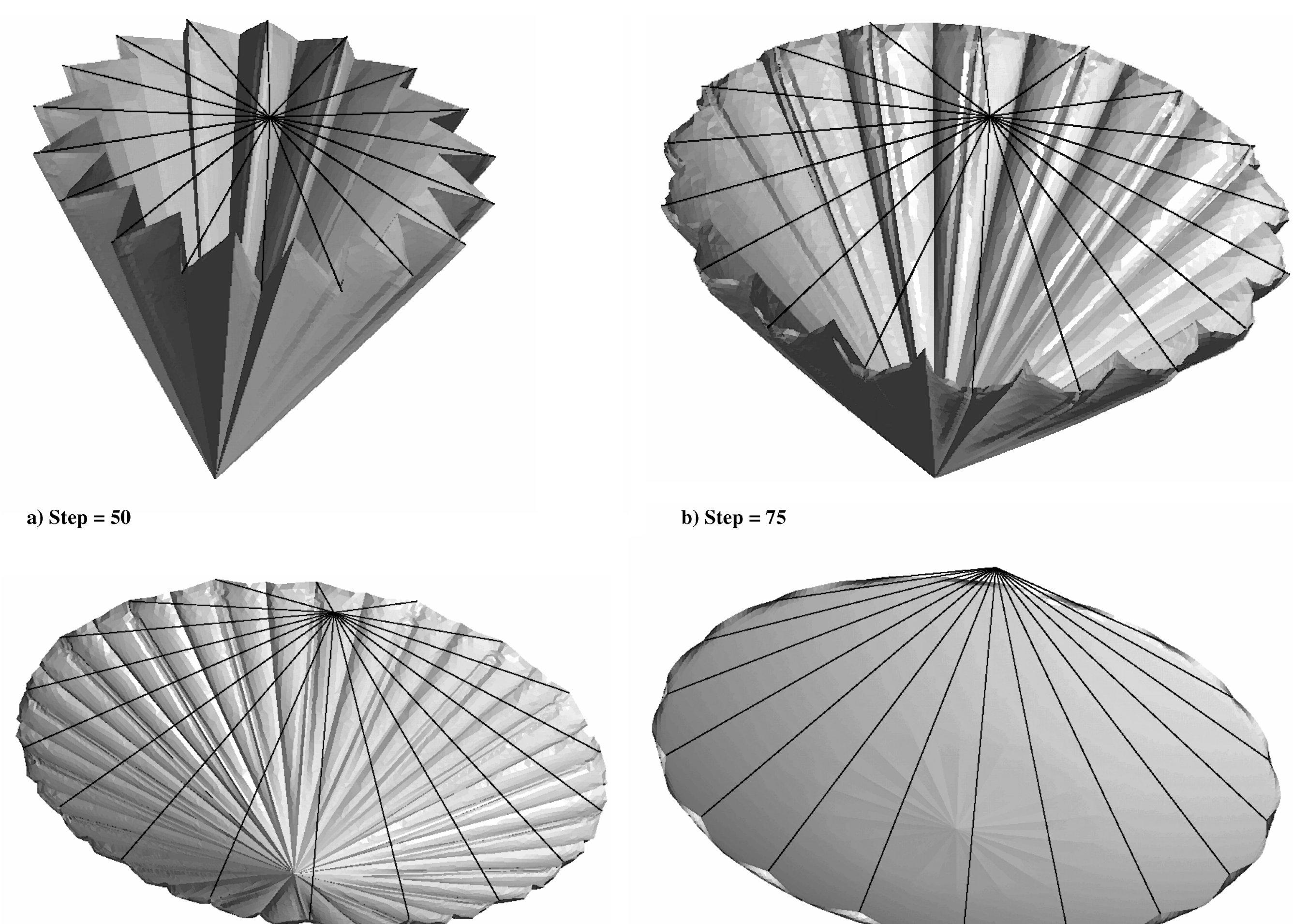

a) Step = 50

b) Step = 75

c) Step = 100

d) Step = 189 (converged)

Fig. 5 Model configurations during Newton–Raphson iteration (with the treatment of wrinkling).

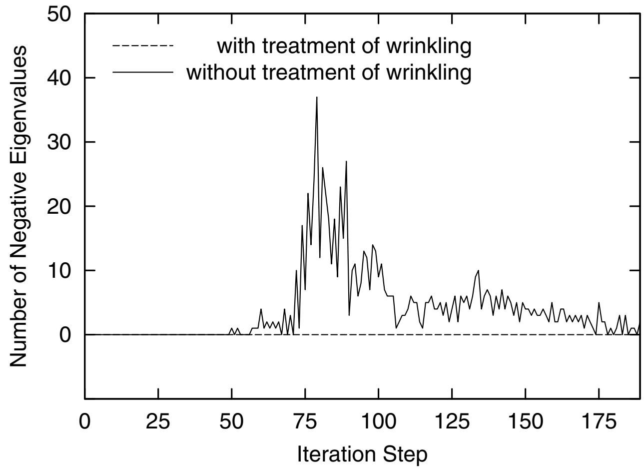

Fig. 6 Comparison of the number of negative eigenvalues of tangent stiffness matrix.

equivalently, when the cable is considered to be tensioned. The reflector is supposed to be constructed from a polyimide (Kapton) membrane of thickness $t = 2.56 \times 10^{-2}$ mm. Young's modulus, Poisson's ratio and the density of the membrane material are given as $E = 2.55 \times 10^9$ Pa, $\nu = 0.34$ and $\rho = 1.42 \times 10^3$ kg/m^3 respectively. The rate of rotation of the antenna system is 0.1 rad/s.

In the numerical calculation, only one gore is considered with appropriate boundary conditions applied. Initially, the gore is folded along the central mast of the antenna system, as shown in Fig. 4. Starting from this initial configuration, the equilibrated configuration of the membrane reflector, when subjected to centrifugal forces, is reached using the usual Newton–Raphson iteration. Because the membrane is initially in tension free state, a stabilization factor is introduced to overcome the underconstrained problem. An initial value of $\mu = 0.14$ is chosen for this example. For comparative study, the problem is addressed with and without the treatment of wrinkling. In the latter case, the membrane is assumed to resist compressive stresses as well as tensile stresses. The load stiffness arising from the centrifugal forces [25] is taken into account in both cases.

Numerical results obtained with the treatment of wrinkling are shown in Fig. 5. The figure shows typical configurations of the numerical model observed during the Newton–Raphson iteration. The iteration process proceeds in a stable manner, converging at the 189th step. Without the treatment of wrinkling, on the other hand, the iteration process suffers from significant instability, and fails to converge (over 2000 trial iterations are performed). The difference between these two results become even clearer when one investigates eigenvalues of the tangent stiffness matrix. Figure 6 shows the number of negative eigenvalues of the tangent stiffness matrix during the iteration process. In the analysis without the treatment of wrinkling, the negative eigenvalues are observed at every step after the first 50 steps. These negative eigenvalues imply the presence of bifurcation points in the vicinity of the configuration assumed by the model at each step. Usually, arclength methods are employed to deal with this type of singularity [26]. However, the methods cannot be applied to this problem, because the initial configuration of the membrane is not on the equilibrium path. In the analysis with the treatment of wrinkling, in contrast, the negative eigenvalues never appear during the whole iteration process; in other words, the tangent stiffness matrix preserves its positive definiteness during the iteration, whereby the convergence of the solution process is guaranteed. It is worth noting that the instability problem cannot be avoided by simply increasing the stabilization factor. For demonstration purposes, we have performed an analysis with a stabilization factor of $\mu = 50.0$ without the treatment of wrinkling. In this analysis, the value of μ is kept constant during the iteration with an attempt to stabilize the solution process. As a result of the larger value of μ, the solution process proceeds in a fairly conservative manner. However, the number of negative eigenvalues suddenly increases at a certain step and the process fails to converge.

B. Example 2: A Pneumatic Membrane Structure

A pneumatic membrane structure shown in Fig. 7 is considered. The structure is fixed to a horizontal support, and subjected to an internal pressure p_0 along with a distributed load f_d on its rectangular top surface. Young's modulus, Poissson's ratio and the thickness of the membrane are given as $E = 2.0 \times 10^8$ Pa, $\nu = 0.3$ and $t = 0.1$ mm, respectively. The internal pressure p_0 is 100.0 Pa. For simplicity, changes in the pressure force due to volumetric change are ignored in this example. A finite element model of the pneumatic membrane structure is shown in Fig. 8, where one quarter of the original structure is discretized with a combination of six-node triangular and nine-node quadrilateral membrane elements. The total number of degrees of freedom is about 28,000.

Finite element calculations are performed in the following manner. First, the inflated shape of the structure, when the internal pressure p_0 alone is applied, is predicted with an introduction of the stabilization factor. Having obtained the inflated shape, the distributed load f_d is applied incrementally to obtain the deformed shape of the structure at each load level. As in the previous example, analysis with and without the treatment of wrinkling are carried out.

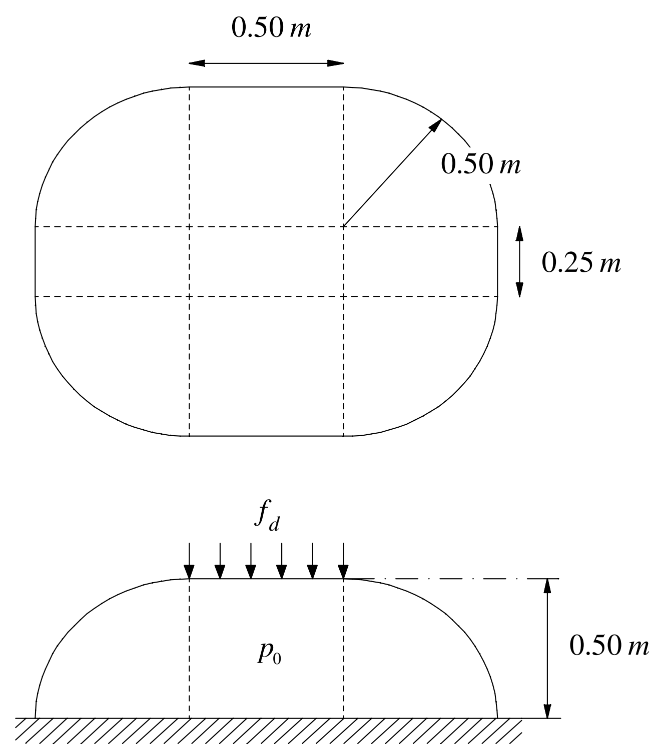

Fig. 7 A pneumatic membrane structure.

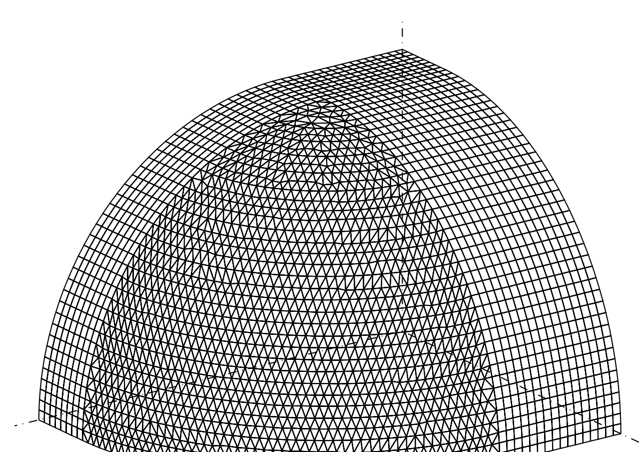

Fig. 8 Finite element model of a pneumatic membrane structure.

In both analyses, the load stiffness resulting from the pressure force [25] is also considered.

Numerical results obtained with and without the treatment of wrinkling are shown in Figs. 9 and 10, respectively. Finite element calculations for the inflated shape are successfully performed in both analyses (Figs. 9a and 10a). Starting from these inflated shapes, the distributed load f_d is incrementally applied for further analysis. In case of the analysis without the treatment of wrinkling, the solution process fails to converge when the load f_d exceeds the value of 160.0 Pa, and no results are available for the deformed shapes beyond this value. In contrast, the analysis with the treatment of wrinkling successfully predicts the deformed shapes for much larger values of f_d (Figs. 9b–9f). During the deformation, several folding lines are observed on the membrane surface. The forming process of these foldings is in itself quite interesting, and should be further investigated in future study.

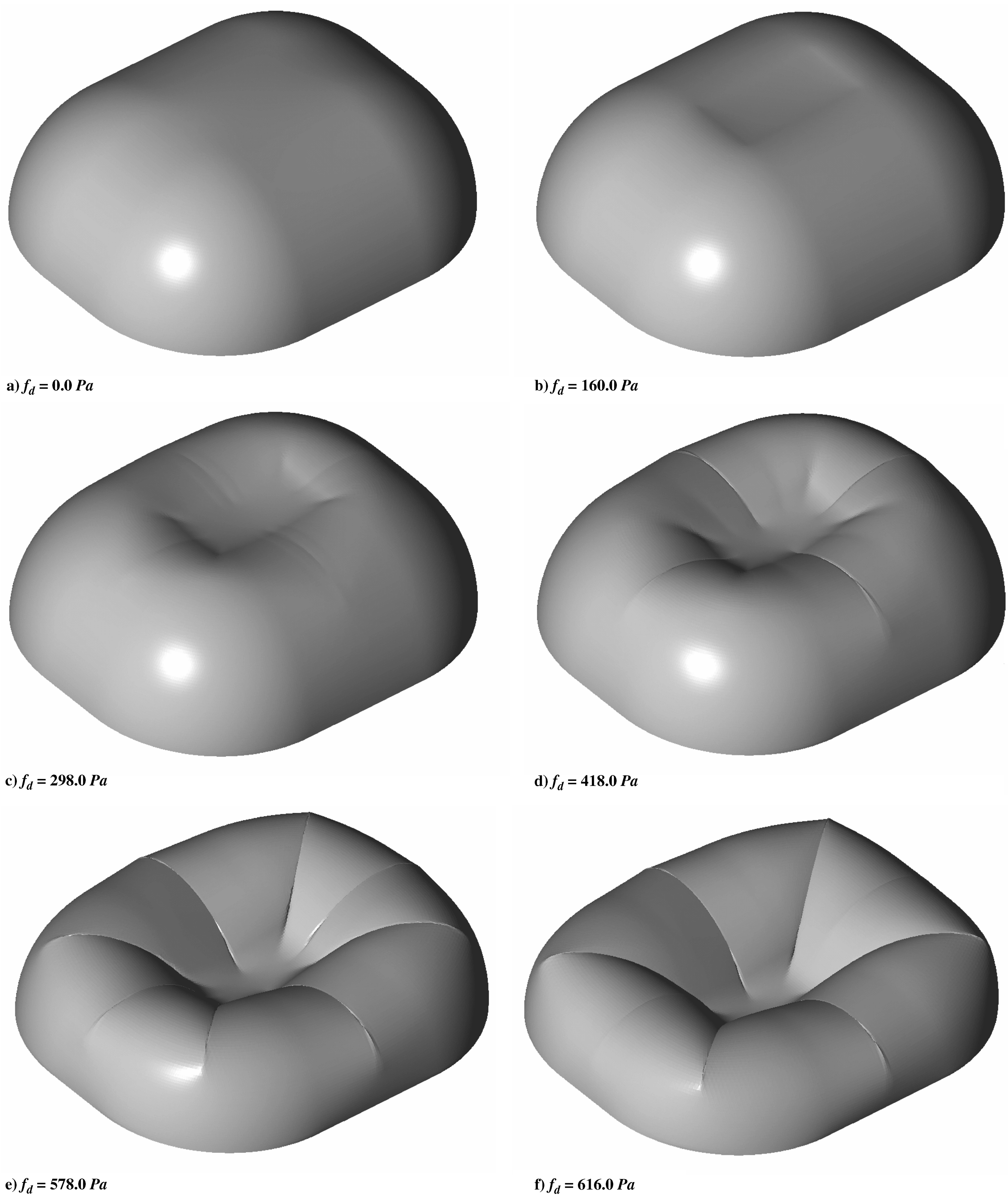

Fig. 9 Deformed configurations of a pneumatic membrane structure (with the treatment of wrinkling).

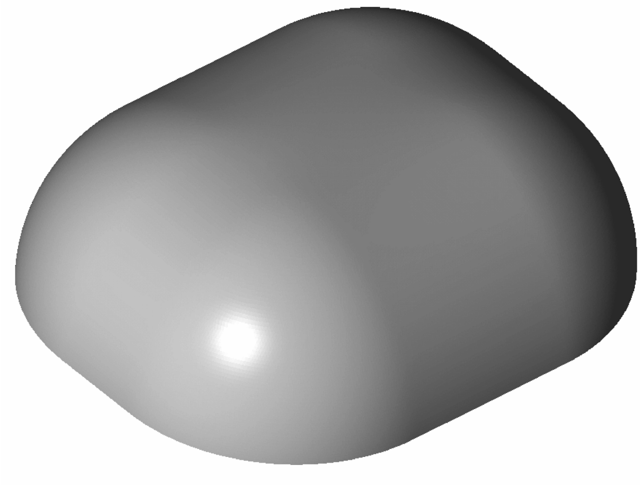

a) f_d = 0.0 *Pa*

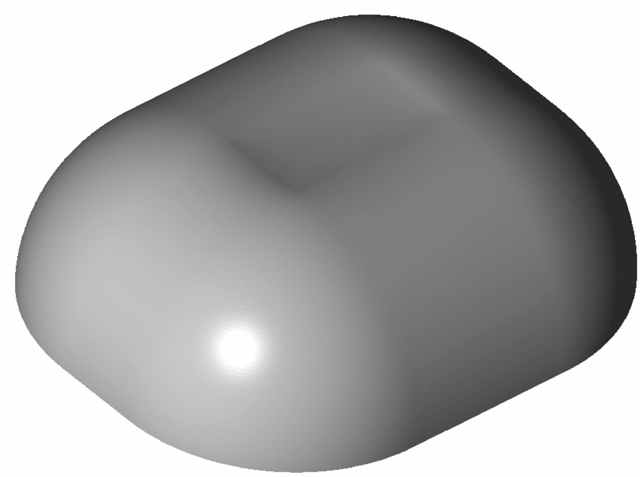

b) f_d = 160.0 *Pa*

Fig. 10 Deformed configurations of a pneumatic membrane structure (without the treatment of wrinkling).

V. Conclusion

The modified stress-strain tensor, recently proposed by the authors to account for wrinkling response of membranes, is applied to three-dimensional membrane problems with the aim to overcome the instabilities usually encountered in finite element analysis using conventional membrane elements. The stabilizing effect of the modified stress-strain tensor is examined through numerical examples. The results show that the use of the modified stress-strain tensor stabilizes the solution process remarkably, and enables one to obtain the converged solution for those problems that are difficult to solve using conventional membrane elements. A numerical investigation of the eigenvalues of the tangent stiffness matrix reveals that the stability provided by the modified tensor is ascribable to the positive definiteness of the tangent stiffness matrix as expected. The calculation algorithm for the modified stress-strain tensor is straightforward and easily implemented with existing finite element codes. With the ease of its implementation, the proposed modification scheme of the stress-strain tensor provides an effective tool not only for wrinkling analysis but also for finite element analysis of membrane structures in general, owing to its stabilizing effect.

References

[1] Reissner, E., "On Tension Field Theory," *Proceedings of the Fifth International Congress for Applied Mechanics*, edited by J. P. den Hartog and H. Peters, Wiley, New York, and Chapman and Hall, London, 1939, pp. 88–92.

[2] Miller, R. K., Hedgepeth, J. M., Weingarten, V. I., Das, P., and Kahyai, S., "Finite Element Analysis of Partly Wrinkled Membranes," *Computers and Structures*, Vol. 20, No. 1–3, 1985, pp. 631–639.

[3] Liu, X., Jenkins, C. H., and Shur, W. W., "Large Deflection Analysis of Pneumatic Envelopes using a Penalty Parameter Modified Material Model," *Finite Elements in Analysis and Design*, Vol. 37, No. 3, 2001, pp. 233–251.

[4] Moriya, K., and Uemura, M., "An Analysis of the Tension Field after Wrinkling in Flat Membrane Structure," *Proceedings of 1971 IASS Pacific Symposium Part 2 on Tension Structures and Space Frames*, Architectural Institute of Japan, Tokyo and Kyoto, 1972, pp. 189–198.

[5] Fujikake, M., Kojima, O., and Fukushima, S. "Analysis of Fabric Tension Structures," *Computers and Structures*, Vol. 32, No. 3/4, 1989, pp. 537–547.

[6] Miyazaki, Y., and Nakamura, Y., "Dynamic Analysis of Deployable Cable-Membrane Structures with Slackening Members," *Proceedings of 21st International Symposium on Space Technology and Science*, 21st ISTS Publication Committee, Omiya, Japan, 1998, pp. 407–412.

[7] Adler, A. L., Mikulas, M. M., and Hedgepeth, J. M., "Static and Dynamic Analysis of Partially Wrinkled Membrane Structures," AIAA Paper 2000-1810, April 2000.

[8] Adler, A. L., and Mikulas, M. M., "Application of a Wrinkled Membrane Finite Element Approach to Advanced Membrane Structures," AIAA Paper 2001-4646, Aug. 2001.

[9] Johnston, J. D., "Finite Element Analysis of Wrinkled Membrane Structures for Sunshield Applications," AIAA Paper 2002-1456, April 2002.

[10] Roddeman, D. G., Drukker, J., Oomens, C. W., and Janssen, J. D., "The Wrinkling of Thin Membranes: Part 1—Theory," *Journal of Applied Mechanics*, Vol. 54, No. 4, 1987, pp. 884–887.

[11] Roddeman, D. G., Drukker, J., Oomens, C. W., and Janssen, J. D., "The Wrinkling of Thin Membranes: Part 2—Numerical Analysis," *Journal of Applied Mechanics*, Vol. 54, No. 4, 1987, pp. 888–892.

[12] Roddeman, D. G., "Finite-Element Analysis of Wrinkling Membranes," *Communications in Applied Numerical Methods*, Vol. 7, No. 4, 1991, pp. 299–307.

[13] Muttin, F., "A Finite Element for Wrinkled Curved Elastic Membranes, and its Application to Sail," *Communications in Numerical Methods in Engineering*, Vol. 12, No. 11, 1996, pp. 775–785.

[14] Jeong, D. G., and Kwak, B. M., "Complementarity Problem Formulation for the Wrinkled Membrane and Numerical Implementation," *Finite Elements in Analysis and Design*, Vol. 12, No. 2, 1992, pp. 91–104.

[15] Lu, K., Accorsi, M., and Leonard, J., "Finite Element Analysis of Membrane Wrinkling," *International Journal for Numerical Methods in Engineering*, Vol. 50, No. 5, 2001, pp. 1017–1038.

[16] Schoop, H., Taenzer, L., and Hornig, J., "Wrinkling of Nonlinear Membranes," *Computational Mechanics Advances*, Vol. 29, No. 1, 2002, pp. 68–74.

[17] Nakashino, K., and Natori, M. C., "Efficient Modification Scheme of Stress-Strain Tensor for Wrinkled Membranes," *AIAA Journal*, Vol 43, No. 1, 2005, pp. 206–215.

[18] Jenkins, C. H., "Nonlinear Dynamic Response of Membranes: State of the Art—Update," *Applied Mechanics Reviews*, Vol. 49, No. 10, 1996, pp. S41–S48.

[19] Steigmann, D. J., "Proof of a Conjecture in Elastic Membrane Theory," *Journal of Applied Mechanics*, Vol. 53, No. 4, 1986, pp. 955–956.

[20] Barnes, M. R., "Form-Finding and Analysis of Prestressed Nets and Membranes," *Computers and Structures* Vol. 30, No. 3, 1988, pp. 685–695.

[21] Han, S. E., and Lee, K. S., "A Study of the Stabilizing Process of Unstable Structures by Dynamic Relaxation Method," *Computers and Structures*, Vol. 81, No. 17, 2003, pp. 1677–1688.

[22] Kang, S., and Im, S., "Finite Element Analysis of Wrinkling Membranes," *Journal of Applied Mechanics*, Vol. 64, No. 2, 1997, pp. 263–269.

[23] Hedgepeth, J. M., "Dynamics of a Large Spin-Stiffened Deployable Paraboloidal Antenna," *Journal of Spacecraft and Rockets*, Vol. 7, No. 9, 1970, pp. 1043–1048.

[24] Freeland, R. E., "Survey of Deployable Antenna Concepts," *Large Space Antenna Systems Technology*, CP-2269, Part 1, NASA, 1983, pp. 381–421.

[25] Hibbit, H. D., "Some Follower Forces and Load Stiffness," *International Journal for Numerical Methods in Engineering*, Vol. 14, No. 6, 1979, pp. 937–941.

[26] Crisfield, M. A., *Non-linear Finite Element Analysis of Solids and Structures, Volume 1: Essentials*, Wiley, New York, 2000, Chap. 9.

A. Berman
Associate Editor